BGSG

Volume 58

Research Paper

Correspondence to:
Filippos Valianatos
fvallian@geol.uoa.gr

DOI number:
http://dx.doi.org/10.12681/bgsg.27062

Keywords:
Earthquake, early warning system, on-site, Thessaly, $IV2_p$

Citation:
Spingos, I., Vallianatos, F. and Kaviris, G. (2021), The Scaling of *PGA* with $IV2_p$ and Its Potential for Earthquake Early Warning In Thessaly (Central Greece). Bulletin Geological Society of Greece, 58, 179-199.

Publication History:
Received: 19/05/2021
Accepted: 06/09/2021
Accepted article online: 13/09/2021

The Editor wishes to thank one anonymous reviewer and Dr. Ch. Evangelidis for their work with the scientific reviewing of the manuscript and Ms Emmanouela Konstantakopoulou for editorial assistance.

THE SCALING OF *PGA* WITH $IV2_P$ AND ITS POTENTIAL FOR EARTHQUAKE EARLY WARNING IN THESSALY (CENTRAL GREECE)

Ioannis Spingos[1,2], Filippos Vallianatos[1,2 *], and George Kaviris[1,2]

[1] Section of Geophysics–Geothermics, Department of Geology and Geoenvironment, National and Kapodistrian University of Athens, 15784 Athens, GR

[2*] Institute of Physics of the Earth's Interior and Geohazards, UNESCO Chair on Solid Earth Physics and Geohazards Risk Reduction, Hellenic Mediterranean University Research Center, Crete, GR 73133 Chania, Greece; fvallian@hmu.gr, fvallian@geol.uoa.gr, +302107274360

Abstract

The main goal of an Earthquake Early Warning System (EEWS) is to estimate the expected peak ground motion of the destructive S-waves using the first few seconds of P-waves, thus becoming an operational tool for real-time seismic risk management in a short timescale. EEWSs are based on the use of scaling relations between parameters measured on the initial portion of the seismic signal, after the arrival of the first wave. Herein, using the abundant seismicity that followed the 3 March 2021 M_w=6.3 earthquake in Thessaly we propose scaling relations for PGA, from data recorded by local permanent stations, as a function of the integral of the squared velocity ($IV2_p$). The $IV2_p$ parameter was estimated directly from the first few seconds-long signal window (t_w) after the P-wave arrival. Scaling laws are extrapolated for both individual and across sites (i.e., between a near-source reference instrument and a station located close to a target). The latter approach is newly investigated, as local site effects could have a significant impact on recorded data. Considering that further study on the behavior of $IV2_p$ is necessary, there are indications that this parameter could be used in future on-site single-station earthquake early warning operations for areas affected by earthquakes located in Thessaly, as it presents significant stability.

Keywords: *earthquake; early warning system; on-site; Thessaly; $IV2_p$*

Περίληψη

Ο κύριος στόχος ενός Συστήματος Έγκαιρης Προειδοποίησης Σεισμών (ΣΕΠΣ) είναι η εκτίμηση της μέγιστης αναμενόμενης εδαφικής κίνησης των καταστρεπτικών εγκαρσίων κυμάτων (S) χρησιμοποιώντας τα πρώτα δευτερόλεπτα των επιμήκων κυμάτων (P). Με τον τρόπο αυτόν, τα ΣΕΠΣ μπορούν να λειτουργήσουν ως εργαλείο για τη διαχείριση του σεισμικού κινδύνου σε πραγματικό χρόνο. Τα ΣΕΠΣ βασίζονται στη χρήση νόμων κλίμακας μεταξύ παραμέτρων που υπολογίζονται στην αρχή του σεισμικού σήματος, μετά την άφιξη του πρώτου κύματος και της αναμενόμενης έντασης της δόνησης. Η τελευταία προσδιορίζεται με διάφορους τρόπους, όπως το μέγεθος σεισμού και η μέγιστη εδαφική επιτάχυνση (PGA) των εγκαρσίων κυμάτων. Στη συγκεκριμένη εργασία, προτείνουμε νόμους κλίμακας για την παράμετρο PGA, συναρτήσει του ολοκληρώματος του τετραγώνου της ταχύτητας στα πρώτα δευτερόλεπτα καταγραφής ($IV2_p$), χρησιμοποιώντας σεισμούς από την πρόσφατη ακολουθία στη Θεσσαλία, η οποία σχετίζεται με τον κύριο σεισμό μεγέθους M_w=6.3 στις 3 Μαρτίου 2021. Χρησιμοποιήθηκαν καταγραφές από τοπικούς μόνιμους σταθμούς. Οι νόμοι κλίμακας των δύο παραμέτρων ($IV2_p$ και PGA) εξάχθηκαν τόσο στην ίδια θέση (και οι δύο προσδιορίσθηκαν από κυματομορφές του ίδιου σταθμού), όσο και μεταξύ μίας θέσης αναφοράς και του στόχου ($IV2_p$ στον σταθμό αναφοράς και PGA στον στόχο). Η τελευταία περίπτωση είναι μία νέα προσέγγιση της μεθόδου, με σκοπό τη διερεύνηση της πραγματικής επίδρασης των διαφορών των τοπικών εδαφικών συνθηκών. Λαμβάνοντας υπόψη ότι απαιτείται περαιτέρω μελέτη της συμπεριφοράς των παραμέτρων, υπάρχουν ενδείξεις ότι η παράμετρος $IV2_p$ μπορεί να χρησιμοποιηθεί σε ένα μελλοντικό ΣΕΠΣ στην περιοχή της Θεσσαλίας.

***Λέξεις-Κλειδιά**: σεισμός; σύστημα έγκαιρης προειδοποίησης; Θεσσαλία; $IV2_p$*

1. INTRODUCTION

In Thessaly (Central Greece), urban areas are located near major active faults increasing the threat of strong seismic events, with, possibly, devastating ramifications for financial and industrial activities, as well as the safety of local population. Advances in signal processing, telecommunications and seismology have gradually rendered the concept of a reliable Earthquake Early Warning System (EEWS) not only feasible, but quite reliable as well (Nakamura, 1988; Kanamori et al., 1997; Allen and Kanamori, 2003; Kanamori, 2005; Simons et al., 2006; Allen, 2007; Gasparini et al., 2011; Hloupis and Vallianatos, 2013, 2015; Parolai et al., 2015; Hsu and Nieh, 2020; Brooks et al.,

2021). Damages from an impending strong motion can be reduced by taking mitigation measures suitable for the given warning time (Espinosa-Aranda et al., 1995; Wu et al., 1998; Iannacone et al., 2010; Beltramone and Gomes, 2021). Such an approach is already in operation in Japan (Nakamura, 1988), Taiwan (Wu et al., 1999, 2000), Mexico (Espinosa-Aranda et al., 1995), Italy (Zollo et al., 2006, 2009, 2010; Satriano et al., 2008) and California, USA (Chung et al., 2020). In Greece, a typical EEWS (Satriano et al., 2011) is currently active at a pilot stage (Kapetanidis et al., 2019), by the Seismological Laboratory of the National and Kapodistrian University of Athens (NKUA-SL). The University of Patras implemented an EEWS to monitor the area around the Rion-Antirion bridge (Sokos et al., 2016). The Geodynamic Institute of the National Observatory of Athens (GI-NOA) had installed an EEWS that also integrated alerts for tsunamis in Rhodes (Papadopoulos et al., 2014) and currently operates a trial system in the Eastern Gulf of Corinth, in cooperation with NKUA-SL and the Hellenic Mediterranean University.

An earthquake generates two fundamental types of body-waves: longitudinal (P) and shear (S) waves. The direct P-waves are weaker in amplitude and have a higher velocity than the S-waves. As a result, the difference in velocity can be used to retrieve information about the earthquake from the first wave arrivals and, consequently, predict the effect of the impending destructive secondary waves (Kanamori, 2005). This notion is implemented in practice by typical EEWSs through the investigation of scaling relationship among the Peak Displacement (P_d) of P-waves, the magnitude (M) and the hypocentral (H) or epicentral distance. The Peak Ground Acceleration (PGA) of the S-waves is retrieved from the expected magnitude estimated from P_d (e.g., Wu and Kanamori, 2005; Satriano et al., 2011). This regional approach introduces weaknesses in the system, as the EEWS' accuracy depends on earthquake location uncertainties and, consequently, is greatly affected by the geometry and density of the available seismological networks. This is in addition to inherent errors, such as the reliability of the regression analysis used to determine the scaling relations' coefficients; extrapolation of accurate coefficients might be difficult, considering the large variability in the level of ground motions for events of similar magnitude (Minson et al., 2019).

Another scaling law, previously explored as a proxy for the impending S-wave amplitude, is the relation between the integral of squared velocity estimated from the initial P-wave ($IV2_p$) and a metric of the anticipated shaking (e.g., PGA, M or the seismic intensity).

Specifically:

$$IV2_p = \int_{t_p}^{t_p+t_w} v^2(t)dt \qquad (1)$$

where t_p the P arrival time, t_w the considered signal window and $v(t)$ the signal in velocity terms. It is an alternative to using a P_d relationship and, therefore, leads to practical applications for early warning (Festa et al., 2008). Applications of $IV2_p$ include recordings by deployments of standard seismological instruments (e.g., Brondi et al., 2015; Spallarossa et al., 2019), as well as smartphones (Hsu and Nieh, 2020). This on-site approach has the advantage of eliminating network design factors (such as requiring multiple suitable locations for instrument installation), while being more immediate; essentially, earthquake location is no longer required. An obvious drawback is the effect of a single site and instrument on the accuracy of the EEWS. Furthermore, in the context of an operational on-site system, there is the issue of avoiding S-waves contamination in the t_w window.

On 3 March 2021 a strong M_w=6.3 earthquake struck Thessaly (Koukouvelas et al., 2021; Mavroulis et al., 2021; Papadopoulos et al., 2021). Its location close to the major city of Larisa (approximately 23 km away) and its shallow depth (~7 km) indicated a source with potential to cause extensive damages. However, the highest *PGA*, recorded at station GINA at the outskirts of the city, was ~140 cm/s^2, well below the limit given by the national building code, i.e., ~235 cm/s^2 (EAK, 2003). This event was followed by another strong earthquake with M_w=6.1 (Ganas et al., 2021), located ~10 km NW. The sequence has offered a considerable number of events so far (over 3,500, two months after the first large event), according to the catalogue of NKUA-SL. Epicenters have spread ~30 km to the NW, covering a very extensive area. Foci are generally located shallower than 15 km (Fig. 1). Even though only recent seismicity raised awareness for seismic hazard and risk in the area, there have been several strong and destructive earthquakes over the years, related to complex active faults. Seismic potential near Larisa is predominantly controlled by normal faulting, with ~15-km-long structures striking WNW-ESE (Caputo et al. 1993, 2004; Ganas et al., 2013). Focal mechanisms related to the 2021 sequence support such patterns (Fig. 1). However, the existence of past strong earthquakes indicates a consistent activation of regional fault systems. The city of Larisa itself, was the epicenter of three strong earthquakes between 1600 and 1900, while the broader area of the 2021 sequence witnessed two such events in 1735 and 1766 (Stucchi et al., 2013).

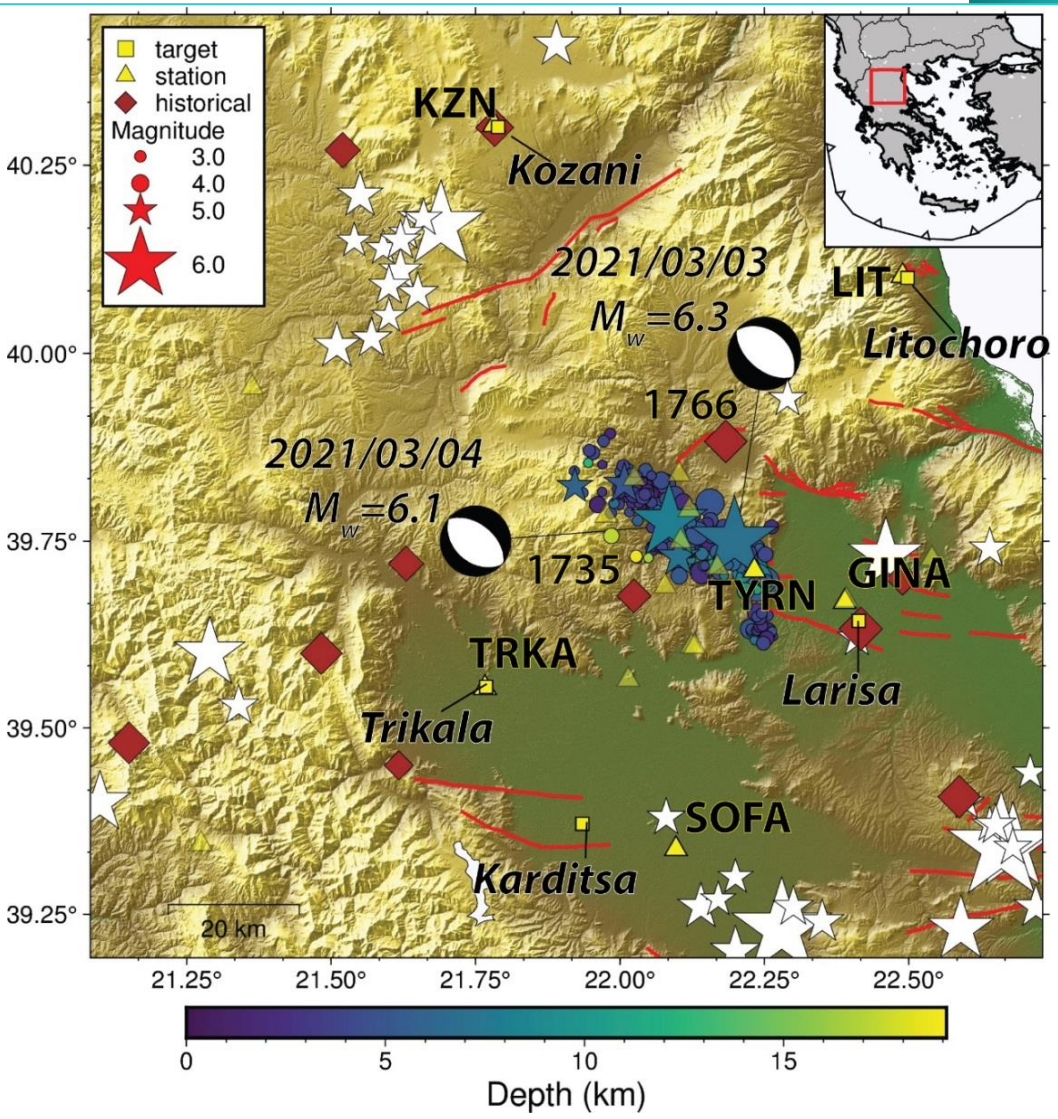

Fig. 1: Seismotectonic setting of the 2021 sequence. Recent seismicity of magnitude equal or greater than 3.0 (circles for magnitudes less than 5.0 and stars for greater) seem to be well-constrained in a ~20-km wide NW-SE linear fashion, in agreement with the strike of nodal planes. Historical earthquakes (brown diamonds) are also observed in the area (Stucchi et al., 2013). The most significant instrumental events (white stars, magnitudes greater than 5.0) is located to the SE and NW, while there is one recorded event within the city of Larisa (Makropoulos et al., 2012; NKUA-SL). Stations used in the study are shown as yellow triangles (instruments not used are faded out). Faults (solid black lines) after Ganas et al. (2013). Focal mechanism solutions from NKUA-SL. Inset: location of the study area (red box).

Considering the uncertainties in methods used for locating historical earthquakes, those earthquakes could well be correlated to the same fault system activated in 2021. Strictly referring to the activated area, there are no significant seismic events since 1766, with the possible exception of a M_w=6.1 shock in 1941 (Makropoulos et al., 2012). The area to the SE has produced a plethora of strong events, with magnitudes exceeding 6.0 (e.g., Papastamatiou and Mouyaris, 1986; Papadimitriou and Karakostas, 2003).

In this work we establish the *PGA-IV2*$_p$ relationship for five target cities in Thessaly: (a) Larisa, (b) Karditsa, (c) Kozani, (d) Trikala and (e) Litochoro. The first four were selected due to their urbanization level, while the last one is a hub for both winter and summer tourism, rendering it a regional financial asset. We exploited the wealth of events that belong to the recent 2021 sequence, as recorded by permanent stations of the Hellenic Unified Seismic Network (HUSN). This is a first step for exploring an on-site EEWS in the region. We explore the relationship between the two quantities both on-site and between a first-trigger station (close to the epicentral area) and each target. Multiple signal windows are investigated to investigate the stability of the laws and identify the possibility of using very short windows to avoid S arrivals within t_w.

2. DATA ACQUISITION AND PROCESSING

To investigate the behavior of *IV2*$_p$ and *PGA* in the area, we used seismic events from the recent 2021 sequence near Larisa. Earthquake information was retrieved from the NKUA-SL, which offers a comprehensive catalogue with manually picked phases. As the available number of events was large (over 2,000) in the one-month period we considered, we selected a cutoff magnitude of 3.0 to include strong signals, as identification of P arrivals could be dubious in weaker events. In total, the selected 1-month-long time period between 03/03/2021 and 03/04/2021 composed a dataset of 206 earthquakes. We then used recordings by HUSN stations that correspond to the sites of interest, i.e., TYRN (calibration near-source velocimeter), GINA (accelerometer located at the outskirts of Larisa), SOFA (accelerometer, available instrument closest to Karditsa, located in Sofades town, 15 km away), KZN (velocimeter at Kozani), TRKA (accelerometer at Trikala) and LIT (velocimeter at Litochoro). These instruments belong to the HL (National Observatory of Athens, Institute of Geodynamics, 1997) and HT (Aristotle University of Thessaloniki Seismological Network, 1981) networks. Station metadata and waveform data were retrieved through the European Integrated Data Archive (EIDA) node at GI-NOA, using the relevant international Federation of Digital Seismograph Network's (FDSN) service (Evangelidis et al., 2021). We used the ObsPy package (Beyreuther et al., 2010; Krischer et al., 2015) to acquire them and process the data.

Concerning data processing, we initially eliminated clipped waveforms, by visual inspection of event-station (velocimeters) pairs of magnitude 4.5 (or greater) and maximum epicentral distance of 30.0 km. Stations with available data, but no manually determined P arrivals, were automatically picked, after filtering the signal between 1 and 20 Hz (Baer and Kradolfer, 1987). Then, using TauP (Crotwell et al., 1999) the S-

P difference time was calculated with a regional velocity model (Karakonstantis, 2017). Finally, preprocessing concluded by removing the instrument's response from the raw data, converting amplitudes to velocity and acceleration, and applying a high-pass filter of 0.075 Hz (Wu and Kanamori, 2005, 2008).

For time windows of 1 s, 2 s and 3 s after the P arrival (t_w), $IV2_p$ was determined. We opted for this range of windows as the calibration station (TYRN) is located very close to the epicenters and, thus, S-P times are small. In any case, if t_w was larger than the theoretically estimated S-P, the event-station pair was rejected. Furthermore, we obtained *PGA* values from a time window starting at the S arrival (either manually determined, if in the initial catalogue, or theoretically by means of the S-P times) and ending 20 s later. We used vertical recordings for estimating $IV2_p$ and horizontal components for *PGA*. Finally, we regressed for the logarithms of the two quantities to estimate linear models of the form:

$$\log(PGA) = a + b * \log(IV2_p) \qquad (2)$$

It is noted that we excluded observations with $\frac{PGA}{P_a} < 2$, where P_a the peak acceleration during t_w. This was necessary to automatically identify and remove incidents of erroneous picking (whether manual or automatic) or ill-determined S-P times (for cases impacted by the uncertainties in the hypocenter, velocity model or ray-tracing algorithm).

After applying the necessary selection criteria, the final dataset consisted of 631 suitable observations for t_w=1 s, 431 for t_w=2 s and 333 for t_w=3 s, amongst the six stations. On average, 65% of the total picks were automatically determined by the Baer and Kradolfer (1987) algorithm. As our study was conducted during the evolution of the sequence, we expected a large number of unpicked (but suitable) arrivals. There seems to be a bias against accelerometers in the catalogue; GINA, SOFA and TRKA had no manually picked observations, after the selection (Fig. 2). However, we note that there were some arrivals determined from these instruments in the initial catalogue (for example, there were 22 picks at GINA that provided ineligible amplitude measurements, as the *PGA* to P_a ratio was less than 2.0). Due to its proximity to the source area, TYRN presented but a few arrivals, especially in longer signal windows (Figs 2b and 2c). LIT, the station with most eligible observations, also featured the highest number of manual picks among all t_w.

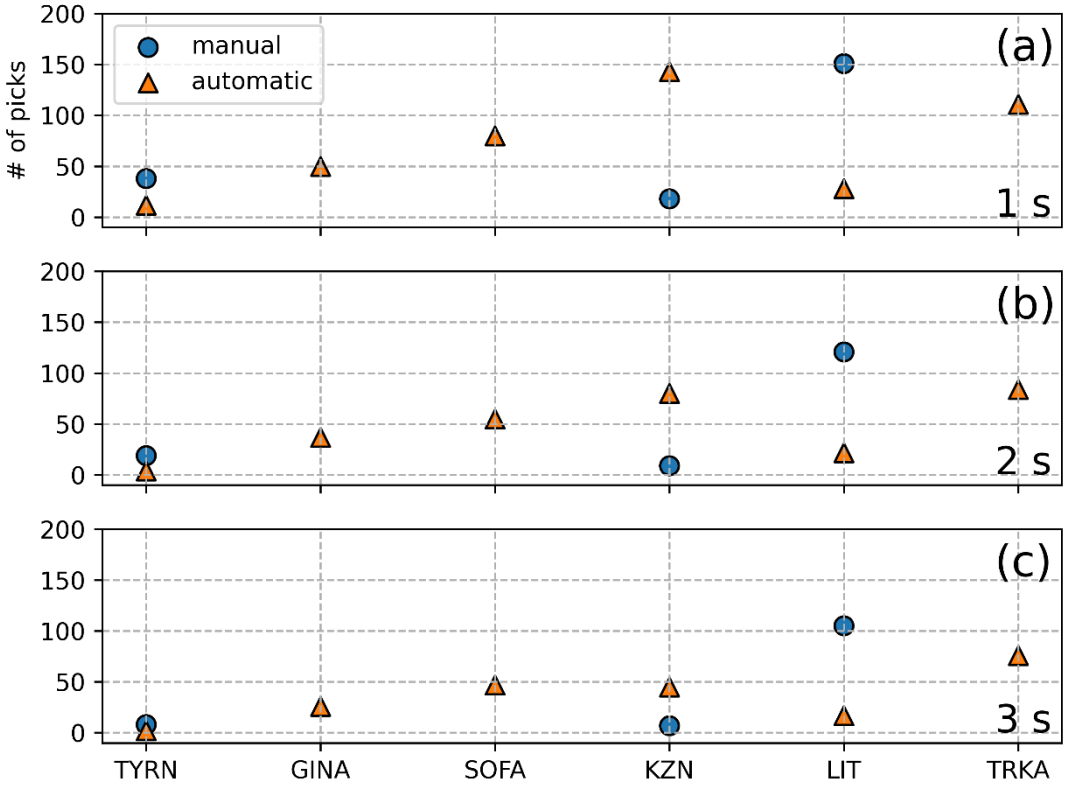

Fig. 2: Distribution of manual (circles) and automatic (triangles) picks corresponding to amplitude observations for each station and signal window, after the application of selection criteria. Each t_w, i.e., 1 s (a), 2 s (b) and 3 s (c), is noted at the bottom right of each subplot.

3. EMPIRICAL CORRELATION LAWS FOR THE AREA OF THESSALY

Determination of the strength of shaking from the initial P-wave are two important elements for earthquake early warning. This can practically be represented by *PGA*, a quantity commonly used in seismic risk and engineering (e.g. Dolce et al., 2020).

3.1. $IV2_p$ as an on-site estimator for *PGA*

As already mentioned, $IV2_p$ has been previously explored as a quantity capable of estimating the earthquake magnitude, with good correlation (Festa et al., 2008). Similarly, our analysis revealed a good correlation between $IV2_p$ and *PGA*, obtained at the same site. Following, we present coefficients of the regression models (as in Eq. 2) for on-site purposes and t_w=2 s (Table 1).

Table 1. Regression results for the on-site analysis and t_w=2 s. a is the intercept, b the slope, σ the individual standard error, N the number of observations in the regression, R^2 the correlation coefficient and SER the standard error of regression.

Station	Site	$a \pm \sigma a$	$b \pm \sigma b$	N	R^2	SER
TYRN	Near source	1.720 ± 0.296	0.334 ± 0.059	23	0.60	0.216
GINA	Larisa	2.320 ± 0.275	0.390 ± 0.047	37	0.67	0.422
SOFA	Karditsa	2.098 ± 0.256	0.372 ± 0.036	55	0.67	0.308
KZN	Kozani	1.677 ± 0.229	0.329 ± 0.032	89	0.55	0.396
LIT	Litochoro	2.133 ± 0.119	0.400 ± 0.018	143	0.80	0.253
TRKA	Trikala	2.023 ± 0.169	0.346 ± 0.025	74	0.70	0.258

For a t_w of 2 s, the intercept of Eq. 2 is constrained between 1.677 and 2.320, while slopes are in the 0.329 to 0.400 range. The two quantities are well-correlated, even though results at KZN suggest a weaker connection. Regression analysis for observations in t_w=3 s offers a higher correlation (between 0.72 and 0.79) from a smaller sample across the board; for instance, suitable observations at TYRN are only 10, due to the proximity to the sources and the very small S-P times. On the other hand, adopting t_w=1 s, yields worse correlation (such as in KZN, where R^2 is 0.285), even though the number of observations is higher. Thus, we consider t_w=2 s as the most balanced window choice, accepting the tradeoff between correlation and data sample size.

Fig. 3 presents *PGA* as a function of $IV2_p$ in TYRN, used as the reference station located near the source. The proximity to most epicenters reduced the number of available observations significantly, as the difference between the arrivals of P- and S-waves was less than 2 s, in most cases. However, measurements obtained by events at the far northern side of the sequence (Fig. 1) provided valuable insight. It seems that a relation between the two quantities can be established in TYRN. In this case, we observe good regression in all time windows (even in 1 s). As seen in Fig. 3, the differences in the coefficients among the t_w are minor. Therefore, using the shortest available t_w to estimate *PGA* from a station that is virtually right above the impending earthquake is not out of the question. Moreover, even in situations such as this, with the closest target being only 23 km away, being able to estimate *PGA* 1 s after the rupture started (and has not even concluded yet) could render $IV2_p$ as the most beneficial and effective EEWS parameter.

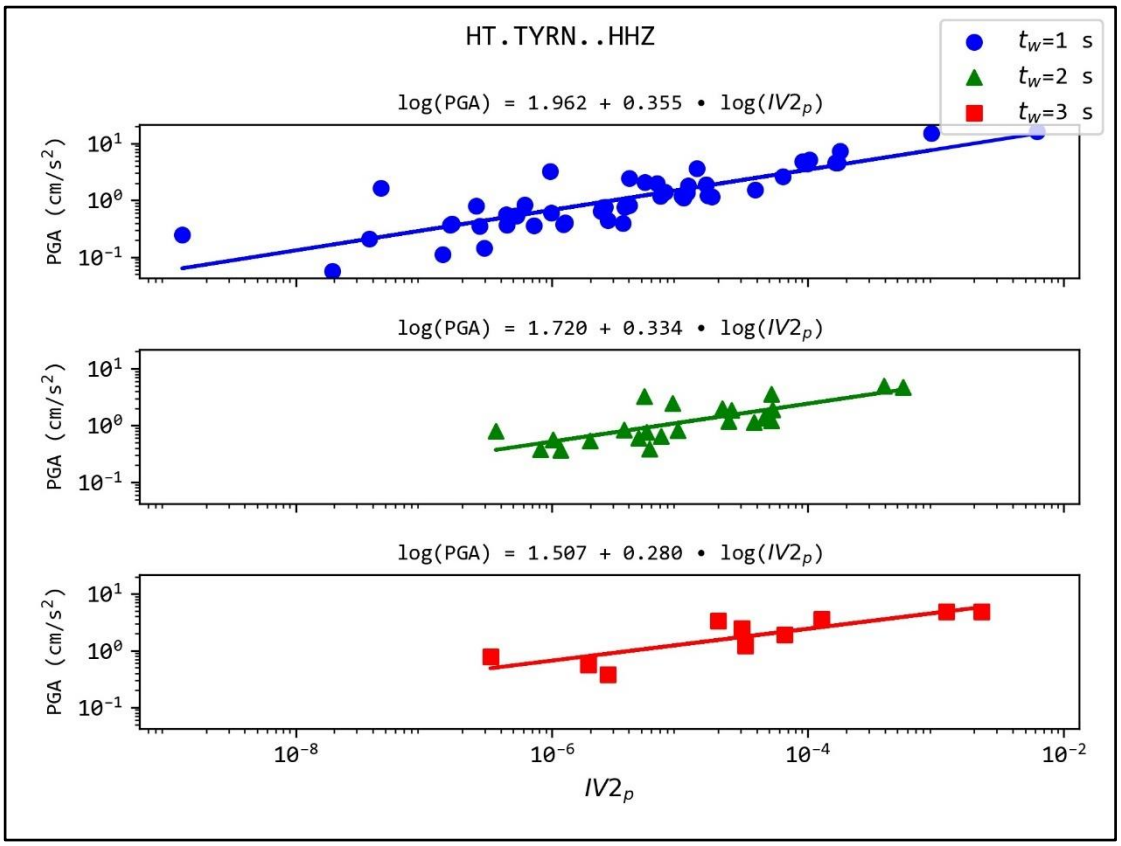

Fig. 3: Regression models of *PGA* for TYRN, in three time windows (t_w) after the P-wave arrival. *PGA* is estimated from the maximum amplitude of the two horizontals after the S-wave arrival, while $IV2_p$ is obtained from the vertical channel.

Similarly, the *PGA* – $IV2_p$ relation showcases good correlation in the target sites Larisa (GINA, Fig. 4a) and Sofades-Karditsa (SOFA, Fig. 4b). At this point, we would like to stress that SOFA was the closest available instrument to Karditsa and we consider this in our interpretation of the results. In any case, both accelerometers document a significantly correlated relation in all signal windows.

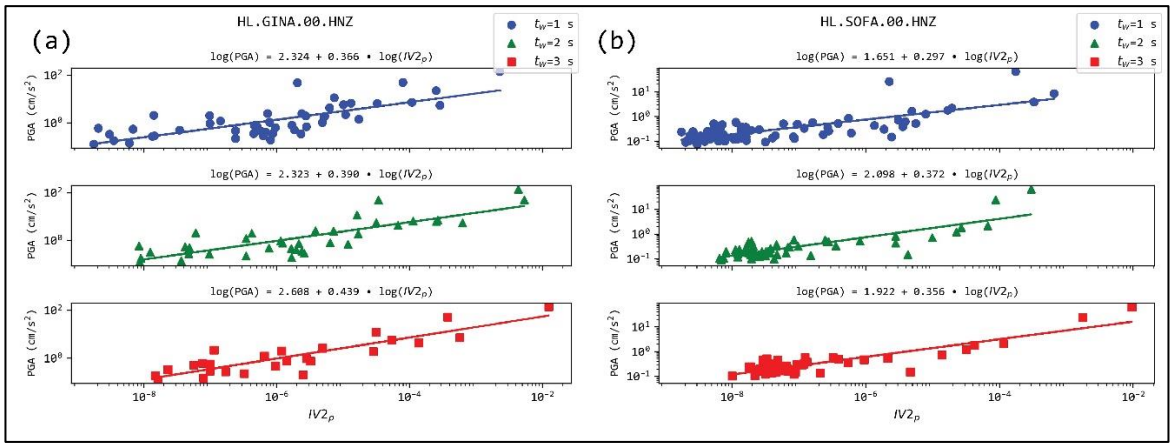

Fig. 4. Regression models of *PGA* for GINA (a) and SOFA (b). Notation as in Fig. 3.

The same behavior is present in the remaining sites, namely Kozani (KZN, Fig. 5a), Trikala (TRKA, Fig. 5b) and Litochoro (LIT, Fig. 5c). The relation between the logarithms of *PGA* and $IV2_p$ is strongly linear. Furthermore, KZN seems to be the station mostly affected by measurements in the 1 s window. There is a group of observations with low $IV2_p$ that deviates greatly from the linear model (Fig. 5a) and leads to significant skewing and low correlation. Nevertheless, the effect of this is eliminated in the 2 s and 3 s windows. Linearity is best shown in LIT (Fig. 5c), a station that, coincidentally, has the largest population of observations.

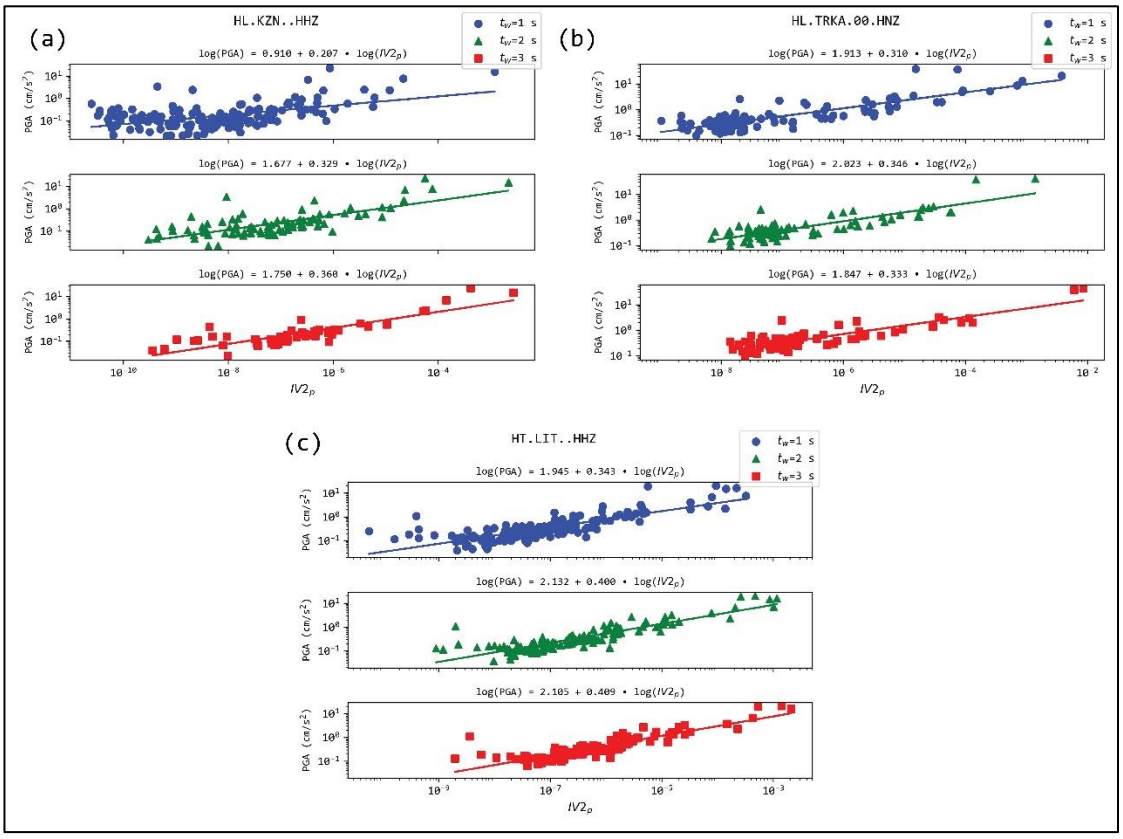

Fig. 5. Regression models of *PGA* for KZN (a), TRKA (b) and LIT (c). Notation as in Fig. 3.

3.2. *PGA* in target sites as a function of near-source $IV2_p$

The concept of using near-source stations to estimate the ferocity of the shaking has been previously explored in literature, by correlation of other parameters with the impending event's magnitude (Wu and Kanamori, 2005; Wu et al., 2007; Zollo et al., 2010). To clarify whether *IV2p* has such a potential, we related measurements of vertical velocity at the reference station located closest to the sequence (TYRN) to PGA at the five target sites (*ts*) (GINA, SOFA, KZN, TRKA and LIT). Essentially, we obtained Eq. 2 between different locations:

$$\log(PGA^{ts}) = a + b * \log\left(IV2_p^{TYRN}\right) \qquad (3)$$

We note that these results are a first approach in researching the feasibility of inter-site relations, between *PGA* and *IV2p*, and are preliminary. Local site effects have not been accounted for and installation sites vary. A clear logarithmic dependence exists with a slope mainly ranging between 0.30 and 0.50, with few exceptions. However, correlation is not as reliable as in the case of the same-site analysis. Inter-site laws for KZN and LIT, two stations north of the target area, presented the lower correlation. It is not yet clear whether this is coincidental or there is a cause, e.g., directivity or distance to the near-source station. In Table 2, we present the regression results for all five sites and t_w=1 s.

Table 2. Regression results for the target analysis and t_w=1 s. Notation as in Table 1.

Station	**Target**	$a \pm \sigma a$	$b \pm \sigma b$	***N***	R^2	***SER***
GINA	Larisa	1.901 ± 0.296	0.324 ± 0.054	18	0.68	0.335
SOFA	Sofades-Karditsa	1.282 ± 0.413	0.320 ± 0.078	15	0.57	0.299
KZN	Kozani	0.069 ± 0.328	0.162 ± 0.058	43	0.16	0.498
LIT	Litochoro	0.720 ± 0.305	0.226 ± 0.054	45	0.29	0.452
TRKA	Trikala	1.177 ± 0.400	0.273 ± 0.078	26	0.34	0.452

Concerning different sites, and taking into consideration the difference in epicentral distance, regression analysis for t_w equal to either 2 s or 3 s did not yield reliable results. The small number of observations for these windows at TYRN acted prohibitively. All regressions (except for LIT and a 2 s window) were carried out with less than 10 observations. Thus, and after considering that a possible connection with a 1 s window at the near-source station would be much more useful, we present regression results for the first window (Table 2). Correlations are much weaker, with only GINA (located 10 km away from TYRN, Fig. 6a) and SOFA (Fig. 6b) exhibiting a satisfactory correlation; yet, it is not as high as the on-site cases. There is no statistically supported connection between TYRN and the other three sites.

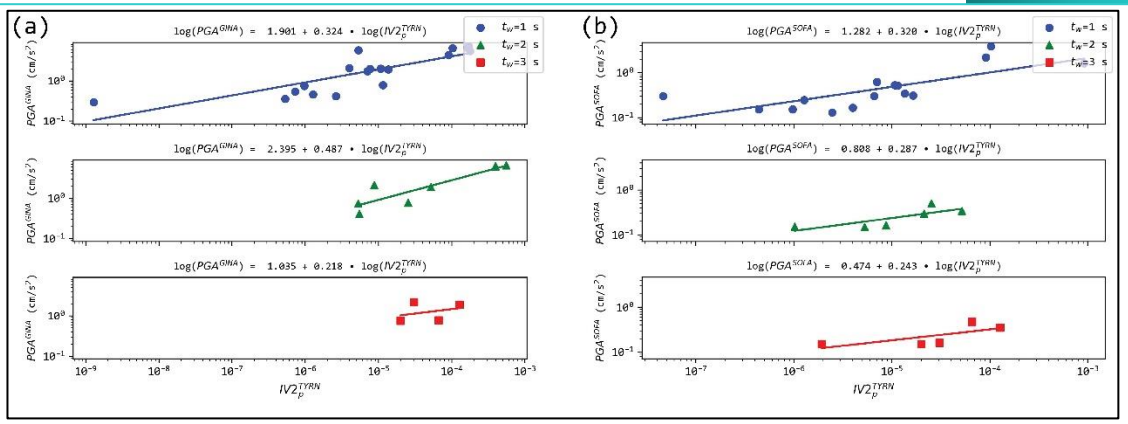

Fig. 6. Regression models of *PGA* between near-source TYRN and targets GINA (a) and SOFA (b). Notation as in Fig. 3.

4. CONCLUSIONS

We estimated empirical scaling relationships between the earthquake early warning parameter $IV2_p$ and *PGA*, using recordings of earthquakes of an extensive sequence in Thessaly which started on March 4, 2021, with the occurrence of a M_w=6.3 event. The earthquake catalogue consisted of 206 events located by NKUA-SL through means of manual phase arrival determination. Waveform data was recorded by permanent stations of HUSN, equipped with velocimeters or accelerometers. The stations were selected to azimuthally cover the area around the activated fault zone, while also correspond to sites of socioeconomic significance. These are Larisa (station GINA), Sofades-Karditsa (SOFA), Kozani (KZN), Litochoro (LIT) and Trikala (TRKA). We also selected an instrument installed at the vicinity of the seismic outburst to use as reference (TYRN). Our findings revealed a linear relationship between the logarithms of $IV2_p$ and *PGA* at single sites, with R^2 being generally greater than 0.60. Signal windows with durations of 2 s and 3 s seem to offer similar correlations, while 1 s seems to be less reliable. The very short duration of the latter renders it more sensitive to errors in phase picking. Moreover, after 1 s, the rupture might still be at a very early stage (for stronger magnitudes M≥6.0). Therefore, out of the three, a t_w of 2 s seems to be the best to estimate *IV2p* as it is long enough to provide good correlation and short enough to include more P-arrivals.

Research on the potential of $IV2_p$ is ongoing, but, if proven fruitful, it can help shape a new landscape for EEWSs, with on-site, front-end design in mind, to increase the lead time and reduce the blind zone. This will permit to grossly estimate the impeding shaking and emit an alert with the expected strong ground motion to affected partners (e.g., government agencies, local industries). The level of seismic hazard in the area

makes the assessment of any developed EEWS and its capabilities extremely useful. Local industrial and other financial activity will greatly benefit from a system that broadcasts alerts, even in short notice, to the sensitive infrastructure of Thessaly. In that aspect, a system that avoids the conundrum of rapid and accurate epicenter and, more importantly, magnitude estimation could be proven invaluable for automating damage mitigation protocols.

In any case, further work is required to establish the spatial (and possibly temporal) behavior of $IV2_p$ and explore its stability both in practical (by application in other areas) and theoretical terms. A model documenting the spatial variation of $IV2_p$ is necessary for operational use. A more modern P-wave picker (e.g., Yanwei et al., 2021) would aid both optimizing the empirical laws and provide a better foundation for estimating the feasibility of the inter-site approach. As S-arrivals would not be known or be able to be estimated in real-time (due to the absence of event locations), a solution needs to be established to avoid shear-wave arrivals in the P signal window. Therefore, further investigation is required on the viability and tradeoff of using a fixed short t_w or employing a real-time S-picker at the near-source station Finally, further investigation should focus in integrating observations from events in a wider magnitude range, by assessing areas where magnitudes greater than 6.0 are present.

5. ACKNOWLEDGMENTS

The authors are grateful to the personnel of the Geodynamic Institute of the National Observatory of Athens and the Department of Geophysics of the Aristotle University of Thessaloniki involved in installing, operating and maintaining the stations used in this study, as well as all staff involved in the Hellenic Unified Seismic Network (recordings of HUSN stations were used by NKUA-SL to determine earthquake locations and focal mechanisms).

The authors would like to express their gratitude to Dr. Christos Evangelidis and an anonymous reviewer for their constructive feedback which greatly improved the manuscript.

We acknowledge support of this study by the project "HELPOS - Hellenic Plate Observing System" (MIS 5002697) which is implemented under the Action "Reinforcement of the Research and Innovation Infrastructure", funded by the Operational Programme "Competitiveness, Entrepreneurship and Innovation" (NSRF

2014-2020) and co-financed by Greece and the European Union (European Regional Development Fund).

Fig. 1 was plotted with GMT 6.0 (Wessel et al., 2019) and its Python wrapper (Uieda et al., 2021). Figs 2 through 6 were plotted with Matplotlib (Hunter, 2007).

6. REFERENCES

Allen, R. M., 2007. The ElarmS earthquake early warning methodology and its application across California in: P. Gasparini, G. Manfredi, and J. Zschau (Eds.), *Earthquake Early Warning System*, Springer, Berlin, 21– 43 pp. doi: 10.1007/978-3-540-72241-0_3

Allen, R. M., Kanamori, H., 2003. The potential for earthquake early warning in Southern California. *Science*, 300, 786– 789. doi: 10.1126/science.1080921

Aristotle University of Thessaloniki Seismological Network, 1981. Permanent regional seismological network operated by the Aristotle University of Thessaloniki, International Federation of Digital Seismograph Networks, doi: 10.7914/SN/HT.

Baer, M., Kradolfer, U., 1987. An automatic phase picker for local and teleseismic events. *Bull. Seismol. Soc. Am.*, 77, 1437–1445.

Beltramone, L., Gomes R.C., 2021. Earthquake Early Warning Systems as an Asset Risk Management Tool. *CivilEng*, 2, 120-133. doi: 10.3390/civileng2010007

Beyreuther, M., Barsch, R., Krischer, L., Megies, T., Behr, Y., Wassermann, J., 2010. ObsPy: A Python Toolbox for Seismology. *Seismol. Res. Lett.*, 81, 530-533. doi: 10.1785/gssrl.81.3.530

Brondi, P., Picozzi, M., Emolo, A., Zollo, A., Mucciarelli, M. 2015. Predicting the macroseismic intensity from early radiated P wave energy for on-site earthquake early warning in Italy. *J. Geophys. Res. Solid Earth*, 120, 7174– 7189. doi: 10.1002/2015JB012367

Brooks, B.A., Protti, M., Ericksen, T., Bunn, J., Vega, F., Cochran, E.S., Duncan, C., Avery, J., Minson, S.E., Chaves, E., Baez, J.C., Foster, J., Glennie, C.L., 2021. Robust

Earthquake Early Warning at a Fraction of the Cost: ASTUTI Costa Rica. AGU Adv. 2, e2021AV000407. doi: https://doi.org/10.1029/2021AV000407

Caputo, R., Bravard, J.-P., Helly, B., 1993. The Pliocene-Quaternary tecto-sedimentary evolution of the Larisa plain (eastern Thessaly, Greece). *Geodin. Acta*, 7, 57–85.

Caputo, R., Piscitelli, S., Oliveto, A., Rizzo, E., Lapenna, V., 2004. The use of electrical resistivity tomography in active tectonics. Examples from the Tyrnavos Basin, Greece. *J. Geodyn.*, 36 (1–2), 19–35.

Chung, A.I., Meier, M.A., Andrews, J., Böse, M., Crowell, B.W., McGuire, J.J., Smith, D.E., 2020. ShakeAlert earthquake early warning system performance during the 2019 ridgecrest earthquake sequence. *Bull. Seismol. Soc. Am.*, 110, 1904–1923. doi: 10.1785/0120200032

Crotwell, H.P., Owens, T.J., Ritsema, J., 1999. The TauP Toolkit: Flexible Seismic Travel-time and Ray-path Utilities. *Seismol. Res. Lett.*, 70, 154–160. doi: 10.1785/gssrl.70.2.154

Dolce, M., Prota, A., Borzi, B., da Porto, F., Lagomarsino, S., Magenes, G., Moroni, C., Penna, A., Polese, M., Speranza, E., Verderame, G.M., Zuccaro, G., 2020. Seismic risk assessment of residential buildings in Italy. *Bull. Earthq. Eng.*, 1–34. doi: 10.1007/s10518-020-01009-5

EAK, 2003. Greek seismic code. Earthquake Planning and Protection Organization, Athens (in Greek).

Espinosa-Aranda, J., Jiménez, A., Ibarrola, G., Alcantar, F., Aguilar, A., Inostroza, M., Maldonado, S., 1995. Mexico City seismic alert system. *Seism. Res. Lett.*, 66, 42–53.

Evangelidis, C., Triantafyllis, N., Samios, M., Boukouras, K., Kontakos, K., Ktenidou, O.J. , Fountoulakis, I., Kalogeras, I., Melis, N., Galanis, O., Papazachos, C.B., Hatzidimitriou, P., Scordilis, E., Sokos, E., Paraskevopoulos, P., Serpetsidaki, A., Kaviris, G., Kapetanidis, V., Papadimitriou, P., Voulgaris, N., Kassaras, I., Chatzopoulos, G., Makris, I., Vallianatos, F., Kostantinidou, K., Papaioannou, C., Theodoulidis, N., Margaris, B., Pilidou, S., Dimitriadis, I., Iosif, P., Manakou, M., Roumelioti, Z., Pitilakis, K., Riga, E., Drakatos, G., Kiratzi, A., Tselentis, G. A., 2021.

Seismic Waveform Data from Greece and Cyprus: Integration, Archival, and Open Access. Seismol. Res. Lett., 92(3), 1672-1684. doi: 10.1785/0220200408

Festa, G., Zollo, A., Lancieri, M., 2008. Earthquake magnitude estimation from early radiated energy. Geophys. Res. Lett., 35, L22307, doi: 10.1029/2008GL035576.

Ganas, A., Oikonomou, I. A., Tsimi, C., 2013. NOAfaults: a digital database for active faults in Greece. *Bul. Geol. Soc. Greece*, 47(2), 518-530. doi: 10.12681/bgsg.11079

Ganas, A., Valkaniotis, S., Briole, P., Serpetsidaki, A., Kapetanidis, V., Karasante, I., Kassaras, I., Papathanassiou, G., Karamitros, I., Tsironi, V., Elias, P., Sarhosis, V., Karakonstantis, A., Konstantakopoulou, E., Papadimitriou, P., Sokos, E., 2021. Domino-style earthquakes along blind normal faults in Northern Thessaly (Greece): kinematic evidence from field observations, seismology, SAR interferometry and GNSS. Bull. Geol. Soc. Greece, 58, 37–86. doi: 10.12681/BGSG.27102

Gasparini, P., Manfredi, G., Zschau, J., 2011. Earthquake early warning as a tool for improving society's resilience and crisis response. *Soil Dyn. Earthquake Eng*., 31(2), 267– 270, doi: 10.1016/j.soildyn.2010.09.004.

Hloupis, G., Vallianatos, F., 2013. Wavelet-based rapid estimation of earthquake magnitude oriented to early warning. *IEEE Geosci. Remote S.*, 10(1), 43-47. doi: 10.1109/LGRS.2012.2191932

Hloupis, G., Vallianatos, F., 2015. Wavelet-Based Methods for Rapid Calculations of Magnitude and Epicentral Distance: An Application to Earthquake Early Warning System. *Pure Appl. Geophys*., 172, 2371–2386. doi: 10.1007/s00024-015-1081-2

Hsu, T.-Y., Nieh, C.P., 2020. On-Site Earthquake Early Warning Using Smartphones. Sensors, 20, 2928. doi: 10.3390/s20102928

Hunter, J.D., 2007. Matplotlib: A 2D Graphics Environment. *Comput. Sci. Eng*. 9, 90–95. doi: 10.1109/MCSE.2007.55

Iannacone, G., Zollo, A., Elia, L., Convertito, V., Satriano, C., Martino, C., 2010. A prototype system for earthquake early-warning and alert management in southern Italy. *Bull. Earthquake Eng.*, 8, 1105–1129. doi:10.1007/s10518-009-9131-8.

Kanamori, H., 2005. Real-time seismology and earthquake damage mitigation. *Annu. Rev. Earth Pl. Sc.*, 33, 195–214. doi: 10.1146/annurev.earth.33.092203.122626

Kanamori, H., Hauksson, E., Heaton, T., 1997. Real-time seismology and earthquake hazard mitigation. *Nature*, 390, 461–464.

Kapetanidis, V., Papadimitriou, P., Kaviris, G., 2019. Earthquake Early Warning application in Central Greece. *Bul. Geol. Soc. Greece*, 7, 95, Ext. Abs. GSG2019-095, 277-278.

Karakonstantis, A. 2017. 3-D Simulation of Crust and Upper Mantle Structure in the Broader Hellenic Area Through Seismic Tomography. Ph.D. Thesis, Department of Geophysics-Geothermics, Faculty of Geology, University of Athens, Athens, Greece.

Krischer, L., Megies, T., Barsch, R., Beyreuther, M., Lecocq, T., Caudron, C., Wassermann, J., 2015. ObsPy: A bridge for seismology into the scientific Python ecosystem. *Comput. Sci. Discov.*, 8, 0–17. doi: 10.1088/1749-4699/8/1/014003

Koukouvelas, I.K., Nikolakopoulos, K.G., Kyriou, A., Caputo, R., Belesis, A., Zygouri, V., Verroios, S., Apostolopoulos, D., Tsentzos, I., 2021. The March 2021 Damasi Earthquake Sequence, Central Greece: Reactivation Evidence across the Westward Propagating Tyrnavos Graben. Geosci., 11(8), 328. doi: 10.3390/GEOSCIENCES11080328

Makropoulos, K., Kaviris, G., Kouskouna, V., 2012. An updated and extended earthquake catalogue for Greece and adjacent areas since 1900. *Nat. Hazards Earth Syst. Sci.*, 12, 1425–1430. doi:10.5194/nhess-12-1425-2012

Mavroulis, S., Mavrouli, M., Carydis, P., Agorastos, K., Lekkas, E., 2021. The March 2021 Thessaly earthquakes and their impact through the prism of a multi-hazard approach in disaster management. Bull. Geol. Soc. Greece 58, 1–36. doi: 10.12681/BGSG.26852

Minson, S.E., Baltay, A.S., Cochran, E.S., Hanks, T.C., Page, M.T., McBride, S.K., Milner, K.R., Meier, M.A., 2019. The Limits of Earthquake Early Warning Accuracy and Best Alerting Strategy. *Sci. Rep.*, 9, 1–13. doi: 10.1038/s41598-019-39384-y

Nakamura, Y., 1988. On the urgent earthquake detection and alarm system (UrEDAS). *Proceeding of 9th world conference on earthquake engineering, Tokyo-Kyoto, Japan.*

National Observatory of Athens, Institute of Geodynamics, 1997. National Observatory of Athens Seismic Network, International Federation of Digital Seismograph Networks, doi: 10.7914/SN/HL.

Papadimitriou, E., Karakostas, V., 2003. Episodic occurrence of strong ($M_w \geq 6.2$) earthquakes in Thessalia area (central Greece). *Earth Planetary Sc. Letters*, 215, 395-409.

Papadopoulos, G., Argyris, I., Aggelou, S., Karastathis, V., 2014. REWSET : A prototype seismic and tsunami early warning system in Rhodes island , Greece, in: Geophysical Research Abstracts, *EGU General Assembly, Vienna, Austria.*

Papadopoulos, G.A., Agalos, A., Karavias, A., Triantafyllou, I., Parcharidis, I., Lekkas, E., 2021. Seismic and Geodetic Imaging (DInSAR) Investigation of the March 2021 Strong Earthquake Sequence in Thessaly, Central Greece. Geosci., 11(8), 311. doi: 10.3390/GEOSCIENCES11080311

Papastamatiou, D., Mouyaris, N., 1986. The earthquake of April 30, 1954, in Sophades (Central Greece*). Geophys. Jour. Inter*., 87(3), 885–895. doi: 10.1111/j.1365-246X.1986.tb01975.x

Parolai, S., Bindi, D., Boxberger, T., Milkereit, C., Fleming, K., Pittore, M., 2015. On-site early warning and rapid damage forecasting using single stations: Outcomes from the REAKT project. *Seismol. Res. Lett.*, 86(5), 1393– 1404, doi: 10.1785/0220140205.

Satriano, C., Lomax, A., Zollo, A., 2008. Real-Time Evolutionary Earthquake Location for Seismic Early Warning. *Bull. Seism. Soc. Am.*, 98 (3), 1482–1494.

Satriano, C., Elia, L., Martino, C., Lancieri, M., Zollo, A., Iannacone G., 2011. PRESTo, the earthquake early warning system for Southern Italy: Concepts, capabilities and future perspectives. *Soil Dyn. Earthquake Eng*., 31 (2), 137-153, doi: 10.1016/j.soildyn.2010.06.008

Simons, F.J., Dando, B., Allen, R. M., 2006. Automatic detection and rapid determination of earthquake magnitude by wavelet multiscale analysis of the primary arrival. *Earth Planetary Sc. Letters*, 250, 214–223.

Sokos, E., Tselentis, G.A., Paraskevopoulos, P., Serpetsidaki, A., Stathopoulos-Vlamis, A., Panagis, A., 2016. Towards earthquake early warning for the Rion-Antirion bridge, Greece. *Bull. Earthq. Eng*., 14, 2531–2542. doi: 10.1007/s10518-016-9893-8

Spallarossa, D., Kotha, S.R., Picozzi, M., Barani, S., Bindi, B., 2019. On-site earthquake early warning: a partially non-ergodic perspective from the site effects point of view. *Geophys. Jour. Inter*., 216(2), 919–934. doi: 10.1093/gji/ggy470

Stucchi, M., Rovida, A., Gomez Capera, A.A., Alexandre, P., Camelbeeck, T., Demircioglu, M.B., Gasperini, P., Kouskouna, V., Musson, R.M.W., Radulian, M., Sesetyan, K., Vilanova, S., Baumont, D., Bungum, H., Fäh, D., Lenhardt, W., Makropoulos, K., Martinez Solares, J.M., Scotti, O., Zivcic , M., Albini, P., Batllo, J., Papaioannou, C., Tatevossian, R., Locati, M., Meletti, C., Viganò, D., Giardini, D., 2013. The SHARE European Earthquake Catalogue (SHEEC) 1000–1899. *J. Seismol*., 17 (2), 523–544. doi: 10.1007/s10950-012-9335-2.

Uieda, L., Tian, D., Leong, W.J., Toney, L., Schlitzer, W., Yao, J., Grund, M., Jones, M., Materna, K., Newton, T., Ziebarth, M., Wessel, P., 2021. PyGMT: A Python interface for the Generic Mapping Tools. doi: 10.5281/ZENODO.4592991

Wessel, P., Luis, J.F., Uieda, L., Scharroo, R., Wobbe, F., Smith, W.H.F., Tian, D., 2019. The Generic Mapping Tools Version 6. *Geochemistry, Geophys. Geosystems*, 20, 5556–5564. doi: 10.1029/2019GC008515

Wu, Y.M., Kanamori, H., 2005. Experiment of an on-site method for the Taiwan Early Warning System. *Bull. Seismol. Soc. Am.*, 95, 347– 353, doi:10.1785/0120040097.

Wu, Y.M., Kanamori, H., 2008. Development of an earthquake early warning system using real-time strong motion signals. *Sensors*, 8 (1), 1– 9.

Wu, Y.M., Shin, T.C., Tsai, Y.B., 1998. Quick and reliable determination of magnitude for seismic early warning. *Bull. Seism. Soc. Am*., 88, 1254–1259.

Wu, Y.M., Chung, J.K., Shin, T.C., Hsiao, N.C., Tsai, Y.B., Lee, W.H.K., Teng, T.L., 1999. Development of an integrated seismic early warning system in Taiwan- case for Hualien earthquakes. *Terr. Atmospheric Ocean. Sci*., 10, 719–736.

Wu, Y.M., Lee, W.H.K., Chen, C.C., Shin, T.C., Teng, T.L., Tsai, Y.B., 2000. Performance of the Taiwan Rapid Earthquake Information Release System (RTD) during the 1999 Chi-Chi (Taiwan) earthquake. *Seismo. Res. Lett*., 71, 338–343.

Wu, Y.M., Kanamori, H., Allen, R., Hauksson, E., 2007. Determination of earthquake early warning parameters, τ_c and P_d, for southern California. *Geophys. J. Int*., 170, 711–717.

Yanwei, W., Xiaojun, L., Zifa, W., Jianping, S., Enhe, B., 2021. Deep learning for P-wave arrival picking in earthquake early warning. *Earthq. Eng. Eng. Vib*., 20, 391–402. doi: 10.1007/s11803-021-2027-6

Zollo, A., Lancieri, M., Nielsen, S., 2006. Earthquake magnitude estimation from peak amplitudes of very early seismic signals on strong motion. *Geophys. Res. Lett*., 33, L23312, doi:10.1029/2006GL027795

Zollo, A., Iannaccone, G., Convertito, V., Elia, L., Iervolino, I., Lancieri, M., 2009. Earthquake early warning system in southern Italy: Methodologies and performance evaluation. *Geophys. Res. Lett.*, 36, L00B07.

Zollo, A., Amoroso, O., Lancieri, M., Wu, Y.M., Kanamori H., 2010. A threshold-based earthquake early warning using dense accelerometer networks. *Geophys. J. Int*., 183, 963– 974, doi:10.1111/j.1365-246X.2010.04765.x